STUDY OF WAVE SOLDERING USING THERMAL-FLUID STRUCTURE INTERACTION TECHNIQUE ON PIN THROUGH HOLE IN PRINTED CIRCUIT BOARD

MOHD SHARIZAL BIN ABDUL AZIZ

UNIVERSITI SAINS MALAYSIA

2015

STUDY OF WAVE SOLDERING USING THERMAL-FLUID STRUCTURE INTERACTION TECHNIQUE ON PIN THROUGH HOLE IN PRINTED CIRCUIT BOARD

by

MOHD SHARIZAL BIN ABDUL AZIZ

Thesis submitted in fulfilment of the requirements

for the degree of

Doctor of Philosophy

August 2015

DECLARATION

I hereby declare that the work reported in this thesis is the result of my own investigation and that no part of the thesis has been plagiarized from external sources. Materials taken from other sources are duly acknowledged by giving explicit references.

Signature: ……..

Name of Student: MOHD SHARIZAL BIN ABDUL AZIZ

Matrix Number: P-CD0004/13(R)

Date: 5th August 2015

ACKNOWLEDGMENT

First and foremost, I would like to express my sincere gratitude and deepest appreciation to my respectable supervisor, Professor Dr. Mohd Zulkifly Abdullah. He provided a good study environment and offered plenty of opportunities for me to explore and pursue my research interest. His encouragement and personal guidance has been instrumental in the concept of the present thesis.

An enormous and great appreciation are also presented to seniors, Dr. C.Y. Khor, Dr. Muhammad Khalil Abdullah, Assoc. Professor Dr. Azman Jalar, Professor Dr. Dadan Ramdan, Mr. Fakhrozi Che Ani, Mr. Nobe Yan, and Mrs Cynthia Cheok for their kind sharing of experience and knowledge towards the success of this research.

My family members have been the largest supporters throughout my PhD research. I am humbly indebted to my loving mother and father, Pn. Rusenah and Mr. Abdul Aziz for their understanding and patience. Special thanks and gratitude to my wife Nor Hana Adam for her patience, encouragement, and continuous support on this research work. To my loving son Muhammad Luth, thanks for being my strength during my study. I wish to express my sincere thanks to my father and mother in law for their continuous support, concern and encouragement which enabled me to complete my PhD.

Thanks as well to all my colleagues who have presented memorable contribution during the preparation of this thesis, namely Syakirin, Najib, Srivalli, Hafiz Jumal, Hafis, Marya, Kamal, Tarmizi, and others. My special thanks also dedicated to staffs at School of Mechanical Engineering USM especially to Mr. Ashamuddin Hashim, for their contribution and effort on my research work.

I gratefully acknowledge the financial support of The Ministry of Higher Education of Malaysia through the My Brain 15 PhD scholarship program, Universiti Sains Malaysia, Universiti Kebangsaan Malaysia, Celestica (Kulim) Sdn. (M) Bhd, Shenzhen Kunqi Xinhua Technology for the technical support and data for this research work. . Last but not least, I gratefully appreciate all those who had helped and supported me in one way or another.

Mohd Sharizal bin Abdul Aziz

August 2015

TABLE OF CONTENTS

Acknowledgment…….. ii

Table of Contents…… iv

List of Tables…….. x

List of Figures……. xii

List of Symbols…… xxii

List of Abbreviations…… xxiv

Abstrak…… xxvi

Abstract…… xxiii

CHAPTER 1 – INTRODUCTION

1.1 Overview…….. 1

1.2 PCB assembly…….. 2

1.3 Wave Soldering Process…….. 3

1.4 Vertical fill and solder joint reliability…… 6

1.5 Problem Statement……... 8

1.6 Research Objective…….. 10

1.7 Scope of the research work…….. 10

1.8 Contribution of study……... 11

1.9 Thesis outline……... 12

CHAPTER 2 – LITERATURE REVIEW

2.1 Overview……..... 13

2.2 Wave Soldering……... 14

2.3 Simulation Modeling…….. 16

2.4 Volume of fluid (VOF) in simulation modeling……. 19

2.5 Wetting…… 20

2.6 PCB warpage and solder joint defect…….. 22

2.7 Optimization – Response surface methodology (RSM)…… 24

2.8 Conclusions…… 27

CHAPTER 3 – METHODOLOGY

3.1 Overview…….. 31

3.2 Description of fluid modeling - FLUENT……... 33

3.2.1 Governing equations……. 35

3.2.1.1 Navier-Stokes equations…… 35

3.2.1.2 Volume of fluid model……... 37

3.2.1.3 Wetting and capillary behavior…….. 38

3.2.2 Modelling and mesh criterion……... 40

3.2.3 Boundary conditions……. 42

3.2.4 Solder material properties……. 44

3.2.5 Simulation setup……... 45

3.3 Description of structural modeling – ABAQUS…….. 47

3.3.1 Modelling and mesh criterion……... 49

3.3.2 Boundary conditions……. 50

3.3.3 Structural mechanical and thermal properties…….. 51

3.3.4 Simulation setup……... 53

3.4 MpCCI coupling method……. 54

3.5 Mesh and time step dependency solution…… 57

3.6 Experimental setup…….. 63

3.6.1 Conventional wave soldering machine……. 64

3.6.2 Introduction of the new adjustable fountain wave soldering machine……. 70

3.6.3 Sample preparation……... 73

3.6.4 Solder filling measurement……... 74

3.6.5 Vertical fill profile…… 75

3.7 Optimization using Response surface methodology (RSM)…… 77

3.8 Case Study – PCB configurations…… 80

3.8.1 Simulation model…….. 80

3.8.1.1 Governing and mathematical equations……. 80

3.8.1.2 Thermal FSI modeling……... 81

3.8.1.3 Fluid modeling……... 82

3.8.1.4 Structural modeling…… 84

3.9 Summary…….. 87

CHAPTER 4 – RESULTS AND DISCUSSION

4.1 Overview……. 88

4.2 Experimental and Simulation validation……. 88

4.2.1 Barrel fill of adjustable wave soldering at different angle…….. 89

	4.2.2	Percentage of barrel fill of adjustable wave soldering at different filling levels……..	91
	4.2.3	Fountain of wave soldering……...	95
	4.2.4	Wetting profile……..	99
	4.2.5	Three dimensional barrel fill profile (Offset angle)……..	102
	4.2.6	PCB temperature profile……...	105
	4.2.7	PTH temperature profile……...	109
	4.2.8	Experimental uncertainty……	112
4.3		Implications of adjustable fountain wave in pin through hole soldering process ……	114
	4.3.1	Effect of conveyor angle and pin shape (PCB thickness: 1.60 mm) ……..	114
	4.3.2	Effect of pin diameter at 1.0 mm PCB hole diameter.....	117
	4.3.3	Effect of PCB thicknesses…….	121
	4.3.4	Voiding in the PTH solder joint……	124
4.4		Fountain flow analysis – Effect of propeller blade…….	129
	4.4.1	Molten solder wave distribution……...	130
	4.4.2	Velocity vector (phase) and filling time	135
	4.4.3	Molten solder wave thickness…….....	138
4.5		Fountain flow analysis - Effects of temperature on the PCB……..	139
	4.5.1	Velocity vector (phase) at full wetting…….	140
	4.5.2	PCB profile at full wetting……	143
4.6		Effect of conveyor angle to the PTH barrel fill……..	146
	4.6.1	Pressure profile…….	148
	4.6.2	Velocity vector……..	153

4.6.3 Selection of conveyor angle…….. 156

4.7 Effect of PTH offset position…….. 157

4.7.1 Filling profile…… 158

4.7.2 Velocity vector at 50% filling and time to full filling….. 162

4.8 Effect of PTH shape…… 164

4.8.1 Molten solder profile at 0.5 s<t<1.5 s……..... 166

4.8.2 Comparison of edge and flat points at 75% filling time……..... 169

4.8.3 Pin filling level at 50% and 75% filling stages……. 172

4.9 Effect of PTH diameter……... 176

4.9.1 Overview of the thermal structure analysis (d/D = 0.2)……..... 177

4.9.2 Temperature distribution on the pin at 0.37 s < t < 1.58 s (d/D = 0.2)…… 179

4.9.3 PTH displacement at 50% and 100% filling level…… 182

4.9.4 Von Mises stress at 50% and 100% filling level…….. 185

4.10 Effect of PTH offset angle…….. 188

4.10.1 Overview of thermal-FSI…….. 189

4.10.2 Pressure distribution……. 191

4.10.3 Temperature profile…….. 193

4.10.4 Pin displacement……... 195

4.10.5 Von Mises stress……... 197

4.11 Optimization of PTH in wave soldering process…… 199

4.11.1 Result of the central composite design……. 201

4.11.2 Regression model equation and analysis of variance (ANOVA)……. 203

4.11.3 Effects of factors on the response……. 206

4.11.4 Optimization of simulation……... 211

4.12 Case Study- Effect of PCB configurations……. 213

4.12.1 Heat transfer coefficient in the wave soldering process (10 s < t < 22 s)……. 215

4.12.2 Displacement of PCB and PTH components in pre-heating (t = 10s) and soldering (t = 22s)……... 218

4.12.3 Von Mises stress at pre-heating (t= 10 s) and soldering (t= 22 s)……. 226

4.13 Summary……. 230

CHAPER 5 – CONCLUSIONS

5.1 Conclusions……. 232

5.1.1 Implications of adjustable wave soldering…….. 233

5.1.2 Fountain flow phenomena and solder pot performances 233

5.1.3 Parametric studies using thermal FSI simulation 234

5.1.4 Optimization using Response Surface Methodology (RSM)……... 236

5.2 Recommendations for future works…… 237

REFERENCES…….. 238

APPENDICES

Appendix A: Calculation of ANOVA analysis……... 248

Appendix B: UDF for wave soldering temperature profile…… 254

PUBLICATIONS LIST 256

LIST OF TABLES

		PAGE
Table 3.1	Sn63Pb37 solder material properties.	45
Table 3.2	Mechanical properties used for the PTH connector.	52
Table 3.3	Thermal properties of PTH connector.	52
Table 3.4	Dimensions of PCB.	52
Table 3.5	Thermal and mechanical properties of FR-4 PCB (Chen and Chen, 2006) (Shen et al., 2005) (Lau et al., 2012a).	53
Table 3.6	Mesh size of soldering pot for mesh-dependency solution.	58
Table 3.7	Summary of grid independence test for fluid meshes.	60
Table 3.8	Summary of grid independence test of structural analysis.	61
Table 3.9	Operation of two-way wave soldering machine.	66
Table 3.10	Actual and coded values for the factor of CCD design.	80
Table 3.11	Material properties used in the PCB configuration.	85
Table 3.12	Thermal properties used in the PCB configuration.	86
Table 4.1	Solder wetting area and discrepancy for both simulation and experiment.	100
Table 4.2	Experimental error of preheating temperature for point 1-4	113
Table 4.3	Experimental error of soldering temperature for point 1-4	113
Table 4.4	Vertical fill volume (%) for circular pin (PCB thickness 1.60 mm).	115
Table 4.5	Vertical fill volume (%) for square pin (PCB thickness	117

	1.60 mm).	
Table 4.6	Average (%) of vertical fill level for adjustable wave soldering machine (square pin).	123
Table 4.7	Average (%) of vertical fill level for conventional wave soldering machine (square pin).	123
Table 4.8	PCB profile (front view).	146
Table 4.9	PTH position.	147
Table 4.10	Offset position.	157
Table 4.11	Maximum and minimum filling level (PCB hole) at t=1.0 s.	168
Table 4.12	Diameter profile (bottom view).	176
Table 4.13	Angle profile (front view).	188
Table 4.14	Offset position.	200
Table 4.15	Diameter profile.	201
Table 4.16	Angle profile (front view).	201
Table 4.17	Results of the central composite design.	203
Table 4.18	ANOVA of quadratic model for filling time at 75% volume (Y1), Von Mises stress (Y2), and maximum displacement (Y3) with the operating parameter. [Offset position (A), pin diameter (B), offset angle (C), and solder temperature (D)].	205
Table 4.19	Minimum value of the responses varied with two of the most influential factors.	211
Table 4.20	The validation of model response and simulation factor, A=0.12mm, B= 0.17 mm, C =0^{o}, D= 473.15 K.	212

LIST OF FIGURES

		PAGE
Figure 1.1	Types of solder joint (a) SMT (b) THT.	3
Figure 1.2	Conventional wave soldering process.	4
Figure 1.3	Double wave soldering process (Martin, 2014).	5
Figure 1.4	Chip wave.	5
Figure 1.5	Lambda wave.	6
Figure 1.6	Vertical fill of solder joint (IPC, 2010); (a) 100% fill. (b) Minimum 75% fill. (c) 50% fill.	7
Figure 2.1	Schematic illustration of wave soldering (Liukkonen at al., 2009, 2011a).	15
Figure 2.2	Wave soldering process (D. W. Coit, Jackson, & Smith, 1998).	15
Figure 2.3	Wetting and Non-wetting phenomenon.	21
Figure 2.4	Percentage of literatures for various topics of study in wave soldering process.	31
Figure 3.1	Research framework.	32
Figure 3.2	Flow chart of fluid modeling.	34
Figure 3.3	Surface tension between solid surface and liquid solder.	39
Figure 3.4	Capillary action of wave soldering.	40
Figure 3.5	3D solder pot meshed model.	41
Figure 3.6	Meshed model of the simulation model.	42
Figure 3.7	Boundary conditions of the computational domain.	43
Figure 3.8	Boundary conditions of the 3-D model for single PTH component.	44

Figure 3.9	Flow chart of structural modeling.	49
Figure 3.10	Structural meshed model.	50
Figure 3.11	ABAQUS meshed model of PTH.	51
Figure 3.12	Basic concept of MpCCI thermal coupling method.	56
Figure 3.13	Overview of MpCCI thermal fluid structure interaction.	56
Figure 3.14	MpCCI simulation flow chart (MpCCI, 2009).	57
Figure 3.15	Mesh-dependency solution of soldering pot; Wetting area (%) vs. Time (s).	59
Figure 3.16	Volume of molten solder versus time for various mesh sizes in fluid analysis.	60
Figure 3.17	Volume of molten solder versus time for various mesh sizes of structural analysis.	62
Figure 3.18	PCBs at different thicknesses (1.6 mm < t < 6.0 mm) used for adjustable fountain and conventional wave soldering process.	64
Figure 3.19	Sample of PCB used for adjustable fountain and conventional wave soldering process. (a) Plain PCB; (b) PCB with PTH components.	64
Figure 3.20	Leaded/ lead free wave soldering machine.	65
Figure 3.21	Wave soldering machine used in experiment.	66
Figure 3.22	Laminar and chip wave of the conventional wave-soldering machine.	67
Figure 3.23	(a) Actual and (b) schematic illustration of experimental setup.	68
Figure 3.24	Circular PTH shape for experimental validation (d=0.3 mm, 0.35 mm, and 0.75 mm).	69
Figure 3.25	Schematic diagram of the adjustable fountain wave soldering machine.	71
Figure 3.26	Schematic illustration of solder pot and pressure nozzles for the adjustable 0^o wave soldering machine.	71

Figure 3.27	Schematic illustration of adjustable pressure nozzles for the adjustable fountain wave-soldering machine.	72
Figure 3.28	Adjustable fountain wave solder from the pressure nozzles.	72
Figure 3.29	Line printed circuit board (PCB).	73
Figure 3.30	Optical microscope used to observe solder profile.	74
Figure 3.31	Sample of PTH component after the sample preparation.	74
Figure 3.32	Alicona InfiniteFocus microscope and the specimen.	75
Figure 3.33	Sample of PCB with PTH components used for adjustable fountain and conventional wave soldering process.	76
Figure 3.34	X-Ray CT scanning machine and specimen of PCB with PTHs.	77
Figure 3.35	PCB configuration.	82
Figure 3.36	FLUENT 3D meshed model.	83
Figure 3.37	Boundary conditions	84
Figure 3.38	PCB configuration.	85
Figure 3.39	3D Structural meshed model	86
Figure 4.1	Validation of experiment and simulation for both adjustable fountain (0^o conveyor angle) and conventional (6^o conveyor angle) wave soldering process.	90
Figure 4.2	PCB hole area covered by the solder from the side view.	91
Figure 4.3	Comparison of experimental and simulation solder profile at 50% and 75% and 100% filling level (0° conveyor angle and 3.1 mm PCB thickness).	92
Figure 4.4	Maximum and minimum filling level.	93
Figure 4.5	Minimum filling level.	94
Figure 4.6	Maximum filling level.	94

Figure 4.7	Simulated and experimental results of flow front advancement at the soldering pot during fountain generation.	95
Figure 4.8	Comparison of flow front advancement at position Z1, Z2 and Z3.	96
Figure 4.9	Comparison of simulation and experimental results. (a) Solder pot (Limits of level X for solder fountain formation) (b) Comparison of molten solder thickness beyond level XX at position Y. (c) Advancement of molten solder at position Y (vertical axis).	97
Figure 4.10	Comparison of simulation and experimental results. (a) Simulation contour and experimental solder area. (b) Solder wetting profile for simulation and experiment.	99
Figure 4.11	Wetting length and fountain advancement of molten solder during the experiment. (a) Solder pot (Limits of level XYZ for solder fountain formation). (b) Contour comparison from side view. (Note: A-PCB wetting distance; B-Maximum fountain advancement. (c) Sn63Pb37 solder advancement; A-PCB wetting distance, B-maximum fountain advancement.	101
Figure 4.12	Comparison of experiment and simulation solder profile at 90% filling level. (a) Detailed view of PCB hole. (b) Overall 3D view.	103
Figure 4.13	Measurement solder profile at position A (depth) = -207.7 μm.	104
Figure 4.14	Comparison of experiment and simulation filling depth at 90% filling level.	104
Figure 4.15	Thermal profile location (Points 1-4).	106
Figure 4.16	Comparison between simulation and experimental measurement. (a) Point 1. (b) Point 2. (c) Point 3. (d) Point 4.	106
Figure 4.17	Thermal profile of simulation and experimental in the wave soldering process on the top of the PCB (including preheating, soldering and cooling).	108
Figure 4.18	Temperature profile at different zones.	110

Figure 4.19	Comparison of ΔT between experiment and simulation.	110
Figure 4.20	ΔT at different solder temperatures.	111
Figure 4.21	Comparison of bottom and top PCB temperatures between experiment and simulation.	112
Figure 4.22	Test samples of circular pin for adjustable fountain (0^o) and conventional (6^o) wave soldering.	115
Figure 4.23	Test samples of square pin adjustable fountain (0^o) and conventional (6^o) wave soldering.	116
Figure 4.24	Average vertical fill volume (%) of circular and square pin at 0^o and 6^o conveyor angle.	117
Figure 4.25	Number of PTH solder joint with topside fillet for 0^o and 6^o conveyor angle. (Number of pin for each PCB =50 samples)	118
Figure 4.26	Test samples for 0^o conveyor angle with different pin diameter.	119
Figure 4.27	Test samples for 6^o conveyor angle with different pin diameter.	120
Figure 4.28	Vertical fill level (%) of adjustable and conventional wave soldering machine.	122
Figure 4.29	Comparison of vertical filling level (%) at different PCB thickness (square pin).	123
Figure 4.30	Number of PTH solder joint with the presence of void. (Number of pin for each PCB =50 samples).	124
Figure 4.31	Examples of void formation on 0^o and 6^o conveyor angle.	125
Figure 4.32	Example of void formation at front view and isometric view.	126
Figure 4.33	Void formation of 3.1 mm PCB thickness.	127
Figure 4.34	Void formation of 6.0 mm PCB thickness for adjustable wave soldering.	128
Figure 4.35	Blade design.	129

Figure 4.36	Cross-sectional view of wave soldering pot at Section 1(S1).	130
Figure 4.37	Comparison wave profile at t = 3.5 s. (a) Isometric view of wave distribution. (b) Cross section view of wave distribution.	131
Figure 4.38	Maximum Filling level (%) at t = 3.5s.	135
Figure 4.39	Velocity vector at 100% filling time.	136
Figure 4.40	Percentage of filling time for various number of propeller blades.	137
Figure 4.41	Fountain advancement or molten solder wave thickness.	139
Figure 4.42	Thickness of fountain advancement.	139
Figure 4.43	Cross-sectional view of wave soldering pot and PCB at Plane 1.	140
Figure 4.44	Velocity vector at full wetting.	141
Figure 4.45	PCB profile (bottom) at full wetting.	144
Figure 4.46	Wetting area (%) vs. Temperature (K).	145
Figure 4.47	Wetting time (s) vs. Temperature (K).	145
Figure 4.48	Cross -sectional view of PCB, and PTH component at plane 1.	148
Figure 4.49	Pressure distribution at t = 1.0 s.	149
Figure 4.50	Effect of conveyor angles to pressure distribution at t=1.0 s.	150
Figure 4.51	Measurement of pressure along A-B and C-D.	151
Figure 4.52	Pressure distribution along A-B and C-D at 75% filling volume for r/R=0.2.	152
Figure 4.53	Pressure distribution along A-B and C-D at 75% filling volume for r/R=0.6.	152
Figure 4.54	Velocity vector at t= 1.0 s.	153

Figure 4.55	Flow front velocity along A-B and C-D at 75% filling volume for r/R=0.2.	155
Figure 4.56	Flow front velocity along A-B and C-D at 75% filling volume for r/R=0.6.	155
Figure 4.57	Maximum velocity along A-B and C-D at 75% filling volume.	156
Figure 4.58	Cross-sectional view of wave soldering pot, PCB, and PTH component at Section 1.	158
Figure 4.59	Effect of offset position to the molten solder advancement (front view).	159
Figure 4.60	Maximum and minimum filling level (percentage) at t= 1.0 s.	161
Figure 4.61	Volume Integral by phase for Sn63Pb37 in percentage at t=1.0s.	161
Figure 4.62	Velocity vector at 50% filling time.	162
Figure 4.63	Time to achieve 50% and 100% of filling.	164
Figure 4.64	Pin through hole (PTH) shape.	165
Figure 4.65	Cross-sectional view of PCB, and PTH component at Plane 1.	165
Figure 4.66	Capillary action profile at 0.5s < t < 1.5s.	167
Figure 4.67	Maximum and minimum filling level (PCB hole) at t=1.0s.	169
Figure 4.68	PCB cross section at 75% of filling Time.	170
Figure 4.69	PCB Cross Section at 75% of filling Time (Point A).	171
Figure 4.70	PCB Cross Section at 75% of filling Time (Point B).	172
Figure 4.71	Measurement of filling level point.	173
Figure 4.72	Pin filling level at 50% and 75%.	174
Figure 4.73	Pin level at 50% filling stage.	174

Figure 4.74	Pin level at 75% filling stage.	175
Figure 4.75	Filling time at 100% of filling stage.	175
Figure 4.76	Cross-sectional view of PCB, PTH component, and solder pot at Section 1.	177
Figure 4.77	Thermal structure profile at t=1.0 s.	178
Figure 4.78	Temperature profile (contour) on pin at 0.37s<t<1.58s.	180
Figure 4.79	Temperature distributions on pin (0.1<d/D<0.95).	181
Figure 4.80	Temperature variations with diameter ration (d/D).	182
Figure 4.81	PTH Displacement at 50% and 100% filling level.	183
Figure 4.82	Displacement along PTH at 100% filling level.	184
Figure 4.83	Maximum displacements on PTH at 50% and 100% filling level.	184
Figure 4.84	Von Mises Stress at 50% and 100% filling level.	186
Figure 4.85	Stress (MPa) along PTH at 100% filling.	187
Figure 4.86	Maximum stresses (MPa) on PTH at 50% and 100% filling level.	187
Figure 4.87	Cross-sectional view of computational domain at A-A.	189
Figure 4.88	Filling level of molten solder (FLUENT) and temperature profile of pin (ABAQUS).	190
Figure 4.89	Pressure distribution at different offset angles.	192
Figure 4.90	Melt front pressure at 75% filling.	193
Figure 4.91	Temperature distribution (unit: K) on pin at 100% filling.	194
Figure 4.92	Temperature distributions on pin at 50%, 75%, and 100%.	195
Figure 4.93	Displacement (unit: mm) on pin at 100% filling.	196
Figure 4.94	Maximum displacement on pin at 50%, 75%, and 100% filling.	197

Figure 4.95	Von Mises stress (unit: MPa) on pin at 100% filling.	198
Figure 4.96	Von Mises stress on pinhead at 100% filling.	199
Figure 4.97	Perturbation plot for (a) filling time at 75% filling, (b) Von Mises stress at 75% filling and (c) maximum displacement at 75% filling. Coded values for each factor are refer to the actual values listed in Table 4.17. (Note: A = offset position, B = pin diameter, C = offset angle, and D = solder temperature).	206
Figure 4.98	3D response surface for (a) filling time, (b) Von Mises stress, and (c) maximum displacement.	210
Figure 4.99	Displacement and von Mises stress of pin after optimization.	212
Figure 4.100	PCB configuration design.	214
Figure 4.101	Comparison of experiment and simulation model; (a) Experiment. (b) Simulation.	214
Figure 4.102	Heat transfer coefficient contour during wave soldering process for configuration 4 board design.	216
Figure 4.103	Heat transfer coefficient at the center of the top PCB during preheating and soldering process for each configuration.	217
Figure 4.104	Maximum heat transfer coefficient.	218
Figure 4.105	Displacement contour for configuration 1-5 during preheating stage.	210
Figure 4.106	Displacement contour for configuration 1-5 during soldering stage.	221
Figure 4.107	Displacement at the center of the top PCB during the preheating and soldering process.	223
Figure 4.108	Maximum displacements during preheating and soldering stage for configurations 1-5 of board design.	224
Figure 4.109	Displacement along BGA component during preheating.	225

Figure 4.110	Displacement along BGA component during soldering.	225
Figure 4.111	Von Mises stress distribution for top and bottom PCB at preheating stage.	227
Figure 4.112	Von Mises stress distribution for top and bottom PCB at soldering stage.	228
Figure 4.113	Von Mises stress at the center of the PCB during the preheating and soldering.	228
Figure 4.114	Maximum Von Mises stress on transistor at soldering stage.	230

LIST OF SYMBOLS

SYMBOL	DESCRIPTION	UNITS
English Symbols		
A	PCB top surface area	m^2
A_{heat}	Surface area for heat transfer by convection	m^2
Bi	Bismuth	-
C_p	Specific heat	J/kg.K
Cu	Copper	-
E	Young modulus	MPa
F	Flow advancement parameter/ volume fraction	-
g	Specific gravity	m/s^2
h	Convection heat transfer coefficient	W/m2.K
k	Thermal conductivity	W/m K
n	Normal plane	-
Ni	Nickel	-
p	Pressure	Pa
q	Convectional heat transfer energy	W
P_{atm}	Atmospheric pressure	Pa
Pb	Lead/Plumbum	-
P_{out}	Outlet pressure	Pa
ΔP	Pressure difference	Pa
R	Universal gas constant	J/mol.K
R_1, R_2	Radii of the curvature on solid surface	m
S	Surface area	m^2
Sn	Tin	-
t	Time	s
T	Local temperature	K or ^oC
Ux, Uy, Uj	Velocity component in x, y, z direction	mm/s
u	Fluid velocity component in x-direction	mm/s
v	Fluid velocity component in y-direction	mm/s
w	Fluid velocity component in z-direction	mm/s
x, y, z	Cartesian coordinates	-

Greek Symbols

η	Viscosity	Pa.s
ρ	Density	kg/m^3
τ	Shear stress	Pa
$\dot{\gamma}$	Shear rate	1/s
γ_s	Surface tension of solid	N/m
γ_l	Surface tension of liquid	N/m
γ_{ls}	Surface tension between liquid and solid surface	N/m
θ	Contact angle	Radiant or degree

LIST OF ABBREVIATIONS

3D	Three dimensional	140
CAD	Computer aided design	82
CCD	Central composite design	154
CFD	Computational fluid dynamics	92
CSM	Cross section microscopy	40
CTE	Coefficient of thermal expansion	310
DSC	Differential scanning calorimetry	40
ENIG	Electroless nickel immersion gold	34
FE	Finite element	66
FR	Flame Retardant	32
FSI	Fluid-structure interaction	123
FV	Finite volume	115
FVM	Finite volume method	70
LS	Low solids	45
OFE	Oxygen free electronics	45
OSP	Organic solderability preservative	34
PCB	Printed circuit board	15
PTH	Pin through hole	15
RMA	Rosin mildly activated	45
RSM	Response surface methodology	111
SD	Sessile drop	44

SEM	Scanning electron microscopy	33
SMM	Surface microetching microscopy	40
SMT	Surface mount technology	2
SOM	Self-organizing map	53
THC	Through hole component	3
THT	Through hole technology	2
TQFP	Thin quad flip package	115
TSOP	Thin small outline package	115
SIMPLE	Semi-Implicit Method for Pressure Linked Equations	81
URF	Under relaxation factor	81
VOF	Volume of fluid	72
WB	Wetting balance	44
X-Ray CT	X-Ray computed tomography	159

KAJIAN BAGI PEMATERIAN GELOMBANG MENGGUNAKAN TEKNIK TERMA-INTERAKSI BENDALIR STRUKTUR KE ATAS PIN TELUS LUBANG DALAM PAPAN LITAR TERCETAK

ABSTRAK

Pematerian gelombang merupakan satu daripada proses yang umum dalam industi pemasangan elektronik di mana ia digunakan untuk menggabungkan komponen pin telus lubang (PTL) ke atas papan litar tercetak (PLT). Kecacatan sambungan pateri seperti retak, pembentukan lompang, dan isian tak lengkap pada lubang PLT menyebabkan kelemahan pada sambungan pateri PTL. Eksperimen tentang pengisian tegak PTL telah dilakukan dengan menggunakan mesin pematerian gelombang boleh laras yang baru (sudut penghantar 0^o). PLT dan komponen-komponen yang sama juga digabungkan dengan menggunakan mesin pematerian gelombang konvensional (sudut penghantar 6^o). Mesin imbasan tomografi sinar-X tak musnah berkomputer pula telah digunakan untuk memeriksa pengisian tegak pada setiap sambungan pateri. Di samping itu, proses pematerian gelombang dengan mempertimbangkan fenomena terma-IBS menjadi fokus kepada penyelidikan ini. Simulasi terma-IBS dilakukan dengan menggunakan perisian isipadu (FLUENT) dan elemen (ABAQUS) terhingga melalui teknik gandingan masa sebenar melalui perisian Mesh-based parallel Code Coupling Interface (MpCCI). Penemuan menunjukkan bahawa pematerian boleh laras memberikan pengisian tegak yang tinggi (~99.4%) berbanding pematerian gelombang konvensional (~90.8%). Selain itu, simulasi diperluaskan kepada beberapa parameter kajian terhadap proses dan faktor rekabentuk seperti sudut penghantar dan geometri PTL (contohnya kedudukan offset, bentuk, diameter, offset sudut). Pengaruh parameter-

parameter ini ke atas agihan aliran bendalir, anjakan struktur, agihan tekanan, dan tegasan telah ditekankan. Tambahan lagi, pengoptimuman penyambung PTL dalam pematerian gelombang juga dilaksanakan dengan menggunakan kaedah sambutan permukaan (RSM) untuk mempelajari hubungan diantara pembolehubah tak bersandar kepada sambutan. Beberapa geometri dan parameter proses untuk PLT dan penyambung PTL yang dioptimumkan menunjukkan ciri-ciri iaitu 0.12 mm kedudukan offset PTL, 0.17 mm diameter PTL, 0^{o} offset sudut dan 473.15 K suhu pateri lebur. Akhir sekali, kajian kes mengenai kesan konfigurasi PLT semasa pematerian gelombang dikaji. Sebanyak lima konfigurasi PLT yang berbeza telah dipertimbangkan Keputusan menunjukkan bahawa konfigurasi komponen PLT mempengaruhi kadar anjakan dan tegasan sesuatu PLT. Pemerhatian daripada keseluruhan kajian ini diharapkan dapat memberi sumbangan yang penting kepada industri mikroelektronik.

STUDY OF WAVE SOLDERING USING THERMAL-FLUID STRUCTURE INTERACTION TECHNIQUE ON PIN THROUGH HOLE IN PRINTED CIRCUIT BOARD

ABSTRACT

Wave soldering is one of the most familiar and well-established processes in the electronics assembly industry, which is used to assemble the pin-through hole (PTH) component onto the printed circuit board (PCB). The solder joint defects such as cracks, void formation, and incomplete filling of the PCB hole may weaken the PTH solder joint. In the present research, the PTH vertical fill was carried out experimentally by using a newly developed adjustable fountain wave soldering machine (0° conveyor angle). A similar PCB and components were assembled by using a conventional wave soldering machine (6° conveyor angle). A non-destructive X-ray computed tomography-scanning machine was employed to inspect the vertical fill of each solder joint. On the other hand, the wave soldering process considering thermal-FSI phenomenon was the focus on this research. The thermal-FSI simulation was carried out by using finite volume (FLUENT) and finite element (ABAQUS) based software through the real time coupling technique using Mesh-based parallel Code Coupling Interface (MpCCI) software. It was found that the adjustable fountain wave soldering yielded higher vertical fill (~99.4%) than the conventional wave soldering machine (~90.8%). Apart from that, the simulations were broadening to the parametric studies on various process and design factors such as conveyor angle and PTH geometry (i.e. offset position, shape, diameter, offset angle). The influences of these parameters on the fluid flow distribution, structural displacement, pressure distribution, and stress have been highlighted. Moreover the

optimization of PTH connector in the wave soldering process using response surface methodology (RSM) was handled to study the interactive relationship between independent variables to the responses. The optimum geometrical and process parameters for the PCB and PTH connector were characterized by 0.12 mm of PTH offset position, 0.17 mm of PTH diameter, 0^{o} of offset angle and 473.15 K of molten solder temperature. Finally the case study on the effects of PCB configuration during wave soldering was investigated. Five PCB configurations were considered based on the position of the components. Results show that PCB component configurations significantly influence the PCB and yield unfavorable deformation and stress. The research findings are expected to be significant contributions in for the microelectronic industry

CHAPTER 1

INTRODUCTION

1.1 Overview

The rapid development in microelectronic technologies presents additional challenges to ensure the reliability and quality of electronic assemblies. High demand in miniature, lightweight, and high-performance electronic products directs the focus toward the reliability of interconnectors between electronic components and printed circuit boards (PCBs). High solder joint reliability provides superior mechanical bonding and functionality of the component. The mechanical strength of the pin through-hole (PTH) component is the reason of implementing through-hole technology (THT) in assembling industries (Berntson et al., 2002). The PTH component is assembled in the wave soldering process, which necessitates particular wave soldering machine to solder PTH onto the printed circuit board (PCB).

The ideal assembly process in wave soldering is to achieve an optimum solder joint result, which does not damage its parts or the assembly in any way and almost zero defect conditions. Definitive design efforts and a proper process control of parameters are required to attain this goal including standardized solder joints, minimum solder spikes or surplus solder, solder skips, bridges, and minimum cleanliness of the assemblies (Bergenthal, 2014; Martin, 2014). Thus, an optimum solder fillet and zero repairs can be achieved. The PCB and component damage due to the over stress and cleaning of the product also can be minimized.

The responsibility of the circuit designer to achieve zero defect PCB and solder joint in the assembly process become challenging by the increasing of component densities, board thicknesses, and fine-pitch devices. An acceptable pin-through hole

solder fillet with practical yields, costs, and process improvement is the key of successful board design (Berntson et al., 2002). The changes in surface finish, increasing power request and reliability issues are also the important issues. Thus, strict requirements on the electronic packaging are needed in the PCB assemblies.

1.2 PCB assembly

Soldering is the most important process in the microelectronics industry. As the demand for electronic products increased, soldering was transformed from the conventional method into machine soldering to improve quality, reliability, and process rate. Reflow and wave soldering are the two main soldering processes involved in surface mount technology (SMT) and through hole technology (THT).

Reflow soldering is the process of attaching surface mount components (SMCs) to PCB (Figure 1.1(a)). The preparatory steps involve screen printing of solder paste to the PCB bond pads, followed by the placement of SMCs on the solder paste deposit. Next, the PCB assembly is subjected to controlled heat in a reflow oven, which melts the solder paste and solder balls and permanently forms the joint (Koch, 1998). The controlled heat in a reflow oven is programmed according to the reflow thermal profile. There are eight output elements of a reflow thermal profile, including preheating slope, soaking temperature, ramp-up slope, peak temperature, and durations of the four heating periods (Lau et al., 2012a; Tsai, 2009). The drawback of using SMT is the failure of solder joint in handling high-power devices especially in military and aerospace industry. These applications need an additional strength to the solder joints (Backwell, 2006).

Thus, the THT was implemented to overcome these problems. The method of attaching pin through-hole (PTH) onto PCB is wave soldering, which is a large-scale soldering process used in through hole component (THC) assemblies. Typically, PCBs with PTHs inserted are pre-fluxed, preheated and then passed over a dual solder wave for soldering (Lee, 2002). The soldered PTH on PCB as illustrated in Figure 1.1(b). The details of the wave soldering process will be discussed in the next subsection.

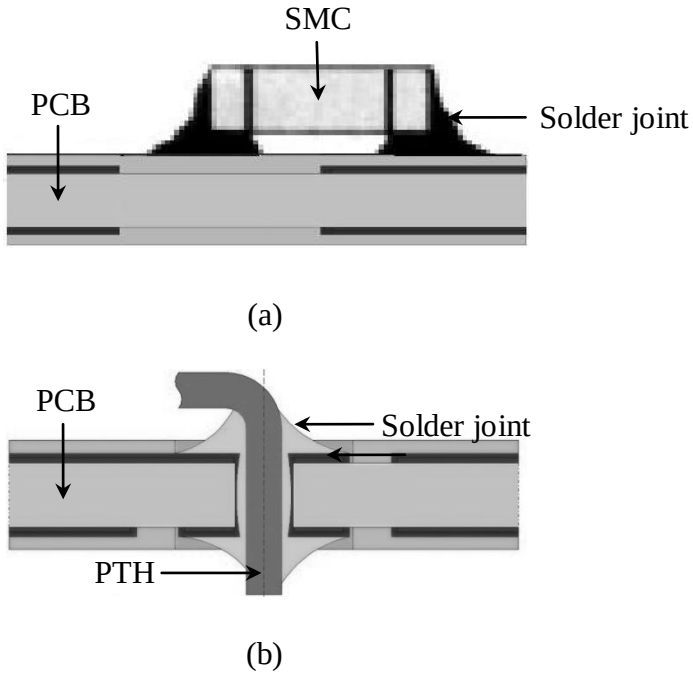

Figure 1.1: Types of solder joint (a) SMT (b) THT.

1.3 Wave Soldering Process

Wave soldering is one of the most widely used soldering methods in the electronics industry, a large-scale process implemented in THC assemblies. The wave soldering machine is used to assemble the PTH components (e.g., capacitor, transistor, and passive components) of a printed circuit board (PCB). This process involves

subsequent stages such as (i) pre-fluxing the PCB with electronic components via flux spray or foam fluxes, (ii) pre-heating, (iii) passing through a single or dual wave for soldering, and (iv) cooling (Lee, 2002). In the wave soldering zone, the PCB with PTH components experience high-temperature molten solder. The bottom surface of the PCB with PTH components interacts with the fountain of the molten solder while the molten solder fills the PCB hole, which is driven by the capillary force of the PCB hole. Afterward, the filled PCB hole is solidified under the cooling zone. Understanding the process parameters of wave soldering, such as temperature, conveyor speed, soldering angle, pre-heating, and cooling zones, is imperative to achieve optimal process conditions. However, different designs of wave soldering machines (e.g., for low- to high-volume production and various zones) may have different optimum process parameter controls. The schematic of the conventional wave soldering process is shown in Figure 1.2.

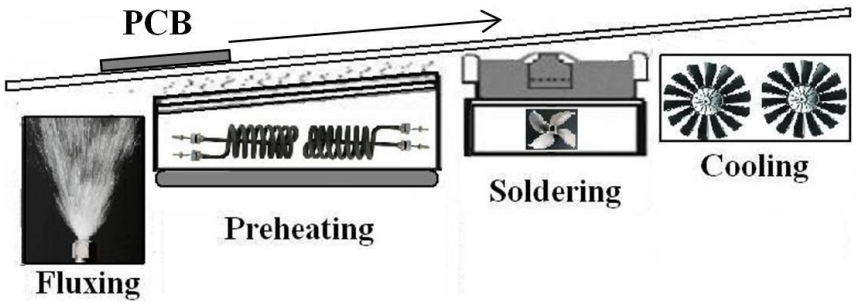

Figure 1.2: Conventional wave soldering process.

In most of the industrial application, dual wave soldering machine has been used to minimize solder joint defect such as incomplete filling, solder bridge, voids, and non-wetting of the lead. The configuration of the dual wave soldering is illustrated in Figure

1.3. The PCB undergoes the primary or ‘chip’ wave with high energy turbulent peak to ensure the molten solder meets every joint of the PTH (Martin, 2014). Next, the PCB passes through a secondary or ‘lambda’ wave, which removes solder bridges or accumulated solder by flow away the excess solder from the PCB. The mechanisms of the chip and lambda wave are shown in Figures 1.4 and 1.5.

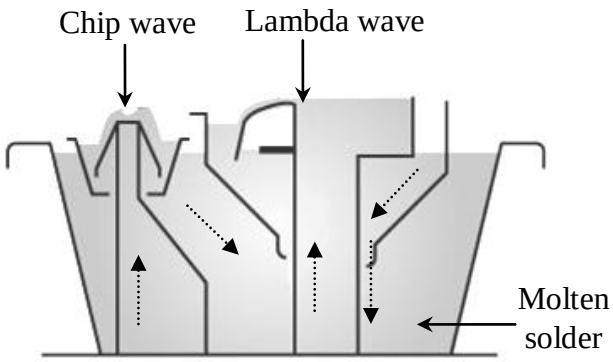

Figure 1.3: Dual wave soldering process (Martin, 2014).

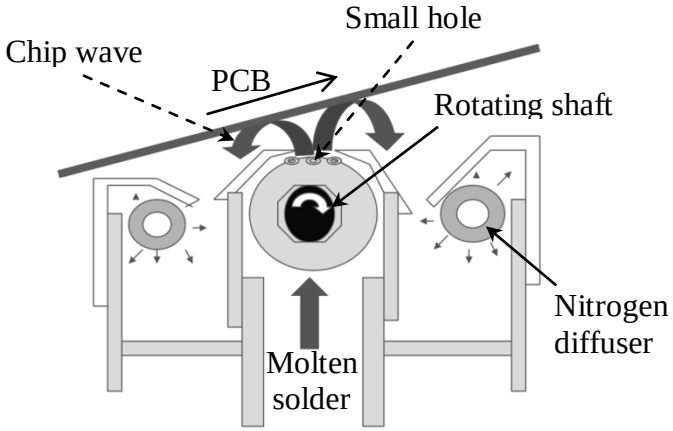

Figure 1.4: Chip wave.

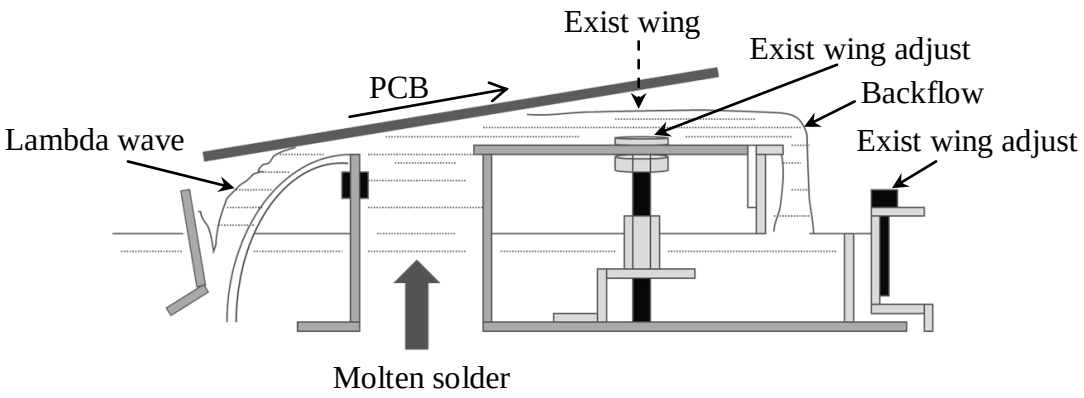

Figure 1.5: Lambda wave.

1.4 Vertical fill and solder joint reliability

In the wave soldering process, the filling of the PCB hole is also known as a vertical fill (IPC, 2010), which is commonly used in the electronics assembly industry. The percentage of vertical fill crucially influences the strength of the solder joint. Therefore, maximum vertical fill (100%) is favored in the wave soldering process as shown in Figure 1.6 (a). Minimum vertical fill at 75% (Figure 1.6(b)) is acceptable; otherwise, the PTH solder joint is considered defective. The vertical fill requirement is strict in applications (e.g., aerospace and military applications) that involve high thermal shock and electrical performance. The solder joint is considered defective when the vertical fill is less than 100% in these applications. However, a vertical fill of 50% (Figure 1.6 (c)) is acceptable under specific conditions when PTH is connected to thermal or conductor layers that function as thermal heat sinks (IPC, 2010). In addition, other problems such as bridging, insufficient topside, and bottom side fillet may lead to short circuit and weak solder joint. Therefore, proper control of process parameters

(Alpha, 2011) (e.g., solder wave height, soldering dwell time, and preheating time) is crucial to eliminate those features on the PTH solder joint.

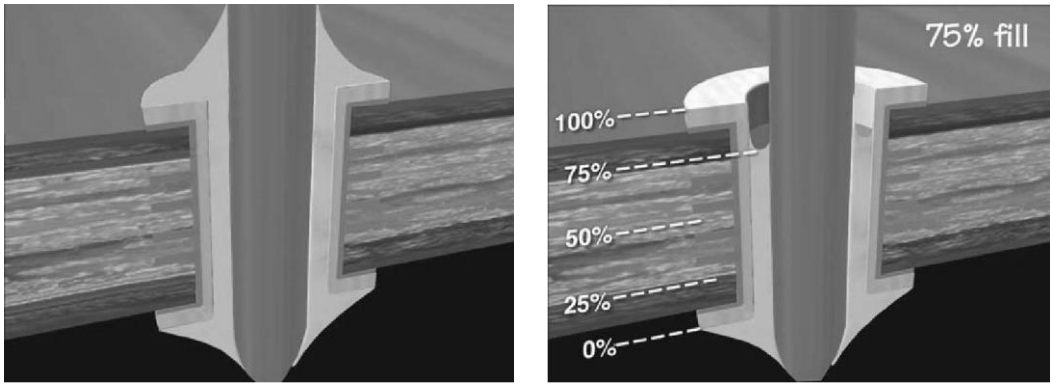

(a) (b)

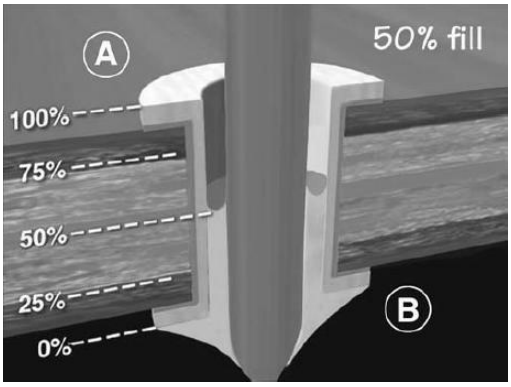

(c)

Figure 1.6: Vertical fill of solder joint (IPC, 2010); (a) 100% fill. (b) Minimum 75% fill. (c) 50% fill.

Solder joint failure typically occurs on the interconnection between a component (e.g., IC package and passive component) and mounting boards (e.g., solder bumps, solder studs, and PTH connectors). The thermal and metallurgical reliability of this solder joint is one of the major issues that hinder the development of small, high-density interconnections (Shi et al., 2014). In addition, the stresses and the displacement caused

by the PTH on solder joints may result in solder joint defects. Improper control of molten solder temperature leads to solder joint fractures when mounting onto the PCB. This situation subjects the PTH to thermo–mechanical stress that exceeds the fracture strength of the solder joint. Moreover, the density and the viscosity of the molten solder also significantly influence the reliability of the wave soldering (Abtew and Selvaduray, 2000). Besides, the molten solder filling characteristics may influence the quality of the solder joint (e.g., unbalanced flow front may induce incomplete filling). Therefore, understanding of molten solder flow characteristics and process visualization is significant for engineers to sustain solder joint reliability.

1.5 Problem Statement

A single or a dual solder pot with a 6° conveyor angle is the typical design of the wave-soldering machine, which is widely used in many industries. Several factors, such as wave solder height, dwell time, and preheating time, have a crucial effect on the vertical filling of the PCB hole. The vertical fill of a PCB hole is always a concern in the electronics assembly process. An increase in PCB thickness may affect the percentage of vertical fill during wave soldering. Conventional wave soldering machines (e.g., single or dual soldering pot) using fountain waveform are typically utilized in the industry. Although wave soldering technology is well established, the vertical fill of the PCB hole still requires proper process control. Several conditions, such as an unstable waveform, insufficient waveform height, improper dwell time, and preheating temperature, may affect the performance of the vertical fill. The molten solder waveform needs proper control to ensure that the stable and sufficient wave solder height interacts with the

bottom surface of the PCB. The non-contact PCB area may result in an unfilled PCB hole.

During wave soldering, the fountain profile generated in a solder pot may affect the PCB hole filling of the component pin/interconnector with PCB, which may result in poor reliability and product rejection. A non-transparent solder pot constrains flow visualization in the solder pot. With the high demand in the microelectronics industry in recent years, the simulation of a coupled FSI becomes an important tool for clear visualization. The key factor to satisfy the geometrical compatibility at the interface between fluid and structure is FSI analysis. Besides, the large scale of the PCB assembly process using wave soldering may cause the thermal mismatch problem due to the different coefficient of thermal expansions (CTEs). The warpage problem leads the other problems such as non co-planarity, chip/component surface cracking, delamination, poor connectivity, and floating. Proper solder material selection is significant to obtain the optimal process performance and soldering reliability in the wave soldering process.

In the PCB assembly, thermal-FSI is involved in wave soldering. The pin-through-hole (PTH) components experience high molten solder temperature while passing through the wave solder pot. High temperature imposed on the pin structure may induce thermal stress and displacement, which may influence the molten solder filling in the PCB hole. The main issue in wave soldering is the reliability and quality of solder joints on the PCB. Examples of solder joint defects are cracks, void formation, and unfilled PCB hole (< 50%). The visualization of a molten solder capillary flowing through PCB is difficult because of the small size of PTH and PCB hole. The intermediate space between PTH and PCB significantly affects capillary flow. Finally,

the development of an electronic assembly industry consumes plenty of time and high cost through the trial and error methods.

1.6 Research Objective

The general idea of wave soldering has been highlighted in the beginning of this chapter. The understandings of the wave soldering process and phenomenon are important to achieve a good quality of the assembled board. Thus, the present study is aimed to fulfill the following objectives:

i. To perform the solder joint filling experiment using the new adjustable fountain (0^o conveyor angle) and conventional (6^o conveyor angle) wave soldering machines.

ii. To investigate the fountain flow phenomena and solder pot performance of the wave soldering process.

iii. To introduce the thermal fluid-structure interaction (FSI) and computational optimization simulation for solving the limitation in the wave soldering process at different processes and physical parameters.

1.7 Scope of the Research Work

In the present research, the study of fluid flow and thermal-FSI within the solder pot, PTH, and PCB are focused on the wave soldering process via the simulation and experiment. The simulation of fluid flow and structural analysis using the thermal-coupling method was focused on the THT assembly by performing in three dimensional model using volume of fluid technique. The validation of the thermal FSI software in solving thermal, fluid flow, and structural behavior is performed with the actual size of

the experimental investigation using the new adjustable fountain and conventional leaded/lead free wave soldering machines. The predicted results were validated with the PCB and PTH thermal profiling data and the visualization of the barrel fill profile obtained from the experiment. This research also aimed to investigate the behaviors of the molten solder through the structures (PTH and PCB) under various parametric case studies to explore the understanding of each factor. In addition, a different physical and process parameters were optimized to achieve the optimum condition using RSM technique and to minimize the thermal stress, deformation, and filling time during the wave soldering process. Finally, the effect of PCB configurations to the components and PCB assembly was performed as the application of the proposed method. The present research work provides fundamental guidelines and references for the thermal coupling method, to enhance understanding of PTH joint issues, capillary flow and to address reliability issues in PCB assembly industries.

1.8 Contribution of study

The contributions of the present research work are listed as follows:

i. This research work provides fundamental knowledge and guideline on thermal-FSI in the wave soldering process.

ii. Implementation of an adjustable fountain (0^o conveyor angle) wave soldering machine and further parametric studies to improve the wave soldering process.

iii. The application of user-defined functions (UDFs) to control the thermal profile of the wave soldering contributes the realistic process condition.

iv. Computational optimization by using response surface methodology contributes in depth understanding of the interactive relationship between process and physical parameter, which improves the performance of the wave soldering process.

1.9 Thesis Outline

This thesis is organized into five chapters. A brief introduction about PCB assembly, wave soldering, vertical fill, problem statement, research objective, scope of the research work, and contribution of the study have been presented in chapter one. Literature review of this research is presented in chapter 2. In chapter 3, the methodology of numerical simulation and experimental is highlighted. The validation of experimental and simulated results, parametric studies, optimization and case study of wave soldering are presented in details in chapter 4. Finally, concluding remarks and recommendation for future works are presented in chapter 5.

CHAPTER 2

LITERATURE REVIEW

2.1 Overview

Wave soldering is a large-scale soldering process used in pin through-hole (PTH) component assemblies. It is an important process in the electronic assembly to solder the components on the printed circuit board (PCB). The pin-through-hole (PTH) components are soldered onto the PCB when passing through the solder pot (Lee, 2002). During the process, the molten solder fills the PCB hole, which driven by the capillary effect. The occupied solder material in PCB hole is solidified in cooling zone and formed the solder joint. The reliability and quality of the solder joint after wave soldering is the most important criteria and become a challenge for engineers and PCB designers. In the manufacturing process, the experiment using trial and error method has been practiced to solve the defects and major issue in wave soldering. Thus, Inagaki et al. (2013) proposed the numerical investigation to observe the vertical fill of wave soldering. This chapter is intended to review the previous works that related to the present research scope. The significant number of previous literatures on the wave soldering is discussed. On the other hand, several topics such as the simulation modeling, flow front advancement, solder material, wetting, PCB warpage and solder joint defect, RSM optimization, and environmental issue are also presented in this chapter. The conclusions of the literature review are presented at the end of this chapter to highlight the research gap in the simulation and experimental work of the wave soldering process.

2.2 Wave Soldering

In electronic assembly, the wave soldering process has been widely utilized in the high-volume soldering of printed circuit boards (PCBs) (Bertiger and Mesa, 1985). The process involves fluxing, preheating, soldering, and cooling. This process is used to solder and assemble the pin through hole (PTH) components (e.g., capacitor, resistor, transistor, and pin connector) onto the PCB. However, components without pin, such as the ball grid array (BGA) integrated circuit (IC) package and leadless component are mounted on the PCB through a reflow soldering process (LoVasco and Oien, 1983). Typically, reflow soldering is performed first to solder the leadless component (e.g., surface mount capacitor and resistor). Then, the process is followed by PTH component placement and the wave soldering process.

During this process, the earlier mounted component and the PCB undergo second thermal loading (Franken et al., 2000) from the high-temperature environment. Improper temperature control in the wave soldering process can induce unintended deformation and stress to the PCB and leadless component. Therefore, understanding the thermal profile and phenomenon during the wave soldering process is essential in minimizing and eliminating the defects or unintended features of PCBs and their components. . Figures 2.1 and 2.2 depict the experimental setups of the wave soldering process that were utilized by Liukkonen et al. (2009; 2011a) and Coit et al., (1998) in their investigations.

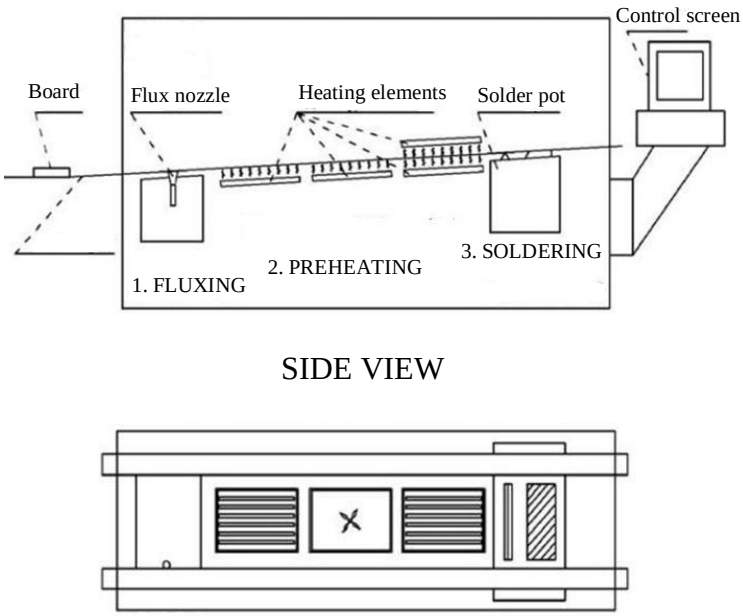

Figure 2.1: Schematic illustration of wave soldering (Liukkonen et al., 2009, 2011a).

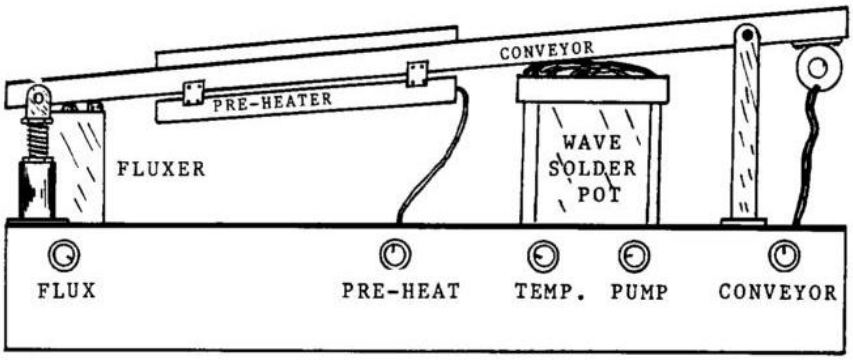

Figure 2.2: Wave soldering process (Coit et al., 1998).

The majority of the wave soldering studies was experimentally conducted. These studies reported on the characteristics of solder materials and mechanical characteristics (Baylakoglu et al., 2005; Kuo et al., 2013), low silver alloy (Wang et al., 2013), self-organizing maps of process optimization (Liukkonen et al., 2009, 2011b), design of

experiment for optimization of materials and process parameters (Arra et al., 2002; Coit et al., 1998; Huang and Huang, 2012), thermal expansion (Fu and Ume 1995), lift-off phenomenon (Suganuma et al. 2000), stress induced by thermal shock (Franken et al. 2000), soldering contact time (Morris & Szymanowski, 2008), the design of the PTH hole (Chang et al., 2011), and gold concentration of the pin (Che Ani et al., 2012), have been reported by several scholars. However, the numerical and simulation studies of the wave soldering process remain a wide research gap and limited literature.

2.3 Simulation Modeling

Simulation analysis plays a significant role in engineering applications, such as in the modeling of biomechanical devices, aircraft structures, automotive components, and microelectronic devices. In recent years, the rapid development of virtual modeling tools has facilitated the efforts of engineers to enhance the reliability of electronic devices. With the aid of simulation modeling technique, the realistic predictions can be achieved through various modeling tools. The modeling tools such as FORTRAN (Abdullah et al., 2007; 2010a), FLUENT (Khor et al., 2011a, 2012a), C-MOLD (Bae et al., 2003; Chan et al., 2004), PLICE-CAD (Hon et al., 2005), Moldex3D (Wang et al., 2010), CAE and FE-based software (Jong et al., 2005; Pei and Hwang, 2005; Teng and Hwang, 2008) had been employed in microelectronics research fields. These modeling tools were mainly used for fluid flow predictions and structural analyses. Optimal design, process setting, and material selection of the wave soldering process can be achieved prior to mass production. Complex governing equations integrated with the volume of fluid (VOF) technique for flow front tracking had been solved by using finite difference method (Hashimoto et al., 2008), finite volume method (Shen et al., 2006;

Wan et al., 2009), and characteristic-based split method in conjunction with finite element method (FEM) (Kulkarni et al., 2006). Modeling tools can also solve complex problems and highly nonlinear problems involved thermal and mass transfer, which are combined with deformation, pressure, and stress on the fluid structure (Kuntz and Menter, 2004).

The experimental work is important in investigating actual problems. The experiment is sometimes limited to specific situations, such as the visualization of deformation, temperature, and stress distribution on the PCB and its components during the process. Tiny PTH and limited equipment have created difficulties in visualizing the real-time PTH filling process. Thus, simulation tools are useful in modeling and simulating the phenomenon of the actual wave soldering process. These tools can also provide the predictive trends of reliability problems. In addition, it is beneficial in small-scale and complex geometry and can minimize the cost of long-term research activity.

In recent years, numerical investigation has enriched the understanding of the wave soldering process (Inagaki et al., 2013). Simulation tool, such as OpenFOAM (Inagaki et al., 2013) have been employed in the study of the wave soldering process. Such study focused on the behavior of the vertical fill of PCB hole. A two-dimensional simple model of the parts was considered in the numerical analysis, which concentrates on the dynamic movement of the molten solder. The numerical simulation study enriched the understanding of the vertical filling mechanism in the wave soldering process by visualizing the molten solder advancement. Aside from the process parameters, the optimized PCB hole and PTH design are the important factors that influence the vertical fill during the wave soldering.

Multi-physics simulation modeling is important to model and solve any phenomenon that involves fluid–thermal and fluid–structural interactions. The fluid and structure is usually treated as a single dynamic element in the direct coupling scheme. The governing equations in each model are integrated simultaneously in the domain (Pironkov, 2009). Furthermore, the thermal FSI analysis may also be utilized to solve highly nonlinear problems (Pironkov, 2009). Thus, a huge amount of computing time is needed for the simulation analysis. Researchers had utilized different boundary formulation methods for the multi-physics simulation. For example, coordinate transformation (Newman and Karniadakis, 1997), moving reference frames (Li et al., 2000), embedded-boundary formulations (Kim et al., 2001; Yang et al., 2005) and non-boundary conforming formulations (Mittal and Iaccarino, 2005). Typically, to solve the multi-physics problem, a coupled simulation is required that enables the simultaneous analysis of either fluid–structure or thermal–structure process. A complex flow field may involve heat and mass transfer combined with the stress, deformation, and pressure distribution of a solid structure (Kuntz and Menter, 2004).

The FSI simulation modeling of the wave soldering process still not reported in the literature. However, several studies had been carried out using the simulation coupling approach to solve the multi-physics problem in electronic packaging. In recent years, the real-time fluid structure interaction (FSI) and thermal-coupling methods had also been employed to solve wire deformation (Ramdan et al., 2011), reflow soldering (Lau et al., 2012b), molded underfill (Khor et al., 2011b; 2012c), and flexible PCB (Leong et al., 2012). Researchers used the MpCCI coupling method to integrate FLUENT and ABAQUS. The simulations were carried out simultaneously, and real-time data transfer was handled by MpCCI software. Although the FSI issue had been

explored in various electronic packaging and assembly processes, there remains a wide research gap in the wave soldering process. Detailed thermal-FSI phenomenon of the electronic assembly process can be revealed by using simulation-modelling technique, which contributes to the understanding of the fundamental and clear visualization of the process

2.4 Volume of fluid (VOF) in simulation modeling

In numerical simulations, the concept of VOF is to track and locate the free surface or fluid to fluid interface in a control volume. The VOF equations can be solved by various discretization methods such as the finite difference (FD), finite element (FE), and finite volume (FV). Typically, the VOF method is utilized to track the flow front advancement, flow profile, and position of the fluid interface. The earlier VOF concept is based on Marker-and-cell (MAC) technique. However, the MAC technique consumes high computational cost and storage requirement (Hirt and Nichols, 1981). Thus, the simple and powerful VOF method was developed which applicable for the 2D and 3D meshes. This method has been integrated in the commercial software to solve the multiphase fluid problems; for example in OpenFoam, ANSYS Fluent, MOLD-FLOW, and CAD-MOLD software. Although the conventional wave soldering technology is widely established in the electronic industry, the in-depth study of the wave soldering using the simulation technique is still lacking in the literature. In recent year, only a few scholars reported the simulation of the wave soldering process. Inagaki et al. (2013) employed OpenFoam software to model the solder filling during the wave soldering process. They only considered a simplified 2D model to investigate the movement of the molten solder. Inagaki et al. (2013) found that the solder volume changes are correlated

to the solder surface configurations when the PTH detach from the solder pot. Besides, the VOF method is also applicable to various engineering problems. For example, the IC encapsulation process (Khor et al., 2012b), wire sweep in plastic ball grid array (PBGA) packaging (Ramdan et al., 2011), multi-stacked chip encapsulation (Ong et al., 2013), stacked chip IC encapsulation (Abdullah et al., 2007; 2010a; 2010b), injection molding (Khor et al., 2010b), biomass and chemical mixing (Sharma et al., 2014).

2.5 Wetting

Wetting is defined as the tendency of molten solder to spread over the PCB. A good wetting is described as the angle formed by the angle of the fluid and surface being soldered at 30^{o} or less on an exposed surface. In wave soldering, a decrease in the contact angle between the PTH and solder is shown by an increase in wetting. A zero contact angle corresponds to spontaneous spreading. Figure 2.3 shows the wetting and non-wetting phenomenon of solder and PCB. According to (IPC, 2010), the acceptance and rejection of solder joint is referred to applicable documentation such as standards, drawings, contracts and references. The criteria of reference documents were classified into three classes which are followed as class 1 class 2, and class 3. For class 1, the criteria requirement is applicable for general electronic products. Class 2 is specified for dedicated service electronic products while class 3 is for high performance electronic products (IPC, 2010). For class 1 and 2 boards, the minimal acceptable solder joint must present 270^{o} of circumferential fillet (IPC, 2010) while the minimal acceptable solder joint for class 3 boards is 330^{o} (Alpha, 2011).

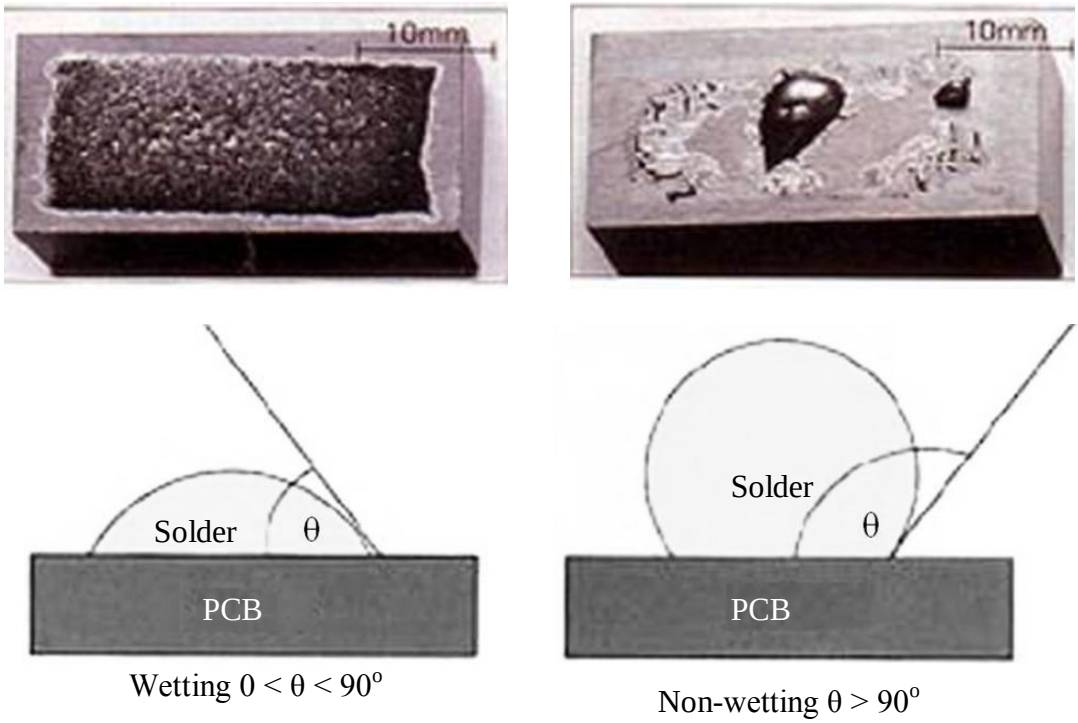

Figure 2.3: Wetting and Non-wetting phenomenon.

The liquidus or melting temperature is identified as the most important factor in wave soldering. The eutectic temperature of Sn–Pb is 183 °C, which is often regarded as the reference temperature. Efficient heat transfer ensures that the solder material melts, forms a joint, and solidifies during the process (Abtew and Selvaduray, 2000). In addition, the wetting and the flowability of the molten solder are determined by the metallurgical bonding between the PTH and the PCB. The temperature of the molten solder affects the surface tension, viscosity, and wetting behavior of the capillary flow during wave soldering. Generating wave solders at varying temperatures may influence the wetting of the PTH within the PCB, which may result in a poor solder joint.

2.6 PCB warpage and solder joint defect

Generally, PCBs undergo different thermal expansions when passed through the wave soldering; this phenomenon leads to thermomechanical fatigue, manufacturing defects, and mechanical catastrophic failure of solder joints (Shen et al., 2006). Warpage occurs when PCB temperature exceeds the temperature of glass transition (Fu and Ume, 1995), and leads to other assembly problems, such as non-co-planarity, solder joint failure, floating, poor connectivity, and chip/component surface cracking (Polsky et al., 2000).

PCB plays an important role in electronic devices and components. PCBs are fabricated from different organic materials that are printed with the circuits, such as polyimide, FR-1, FR-2, FR-4, bismaleimide, and cyanate ester. The complexity of PCBs can be classified into single-sided, double-sided, and multi-layered. Printed circuits provide power and connect the components and the IC package. Moreover, PCBs function as carriers for components and IC packages. In the assembly process, the PCB experiences temperature variations in different assembly stages, such as during reflow and wave soldering. Typically, the temperature at reflow and wave soldering is around 240 °C to 250 °C. During these processes, PCB temperature increases and decreases at each stage. These temperature variations may induce PCB warpage, which is also recognized as out-of-plane displacement (Tan and Ume, 2012). The coefficient of thermal expansion mismatch among the materials results in PCB warpage. PCB warpage is a concern not only for board transfer during automated assembly, but also for the performance of the final assembly, because it may lead to severe joint failures.

Only a few scholars conducted the study on PCB warpage and solder joint defect during the wave soldering. Polsky et al. (2000) investigated PCB warpage caused by

infrared reflow and wave soldering. Two PCB layouts were used to study thermally induced deflection. They observed that both PCBs experienced large deflection (bowl-like shape) in wave soldering, which attributed to the presence of larger through-thickness thermal gradients. The PCB deflection was evaluated by using a shadow Moire pattern (Polsky et al., 2000) . To minimize warpage, Johnson (2014) reported the advantages of a pallet during wave soldering. They introduced high temperature thermoset composite as a solder pallet material. The pallet exposes the particular PCB region (soldering area) to the solder wave, which can minimize PCB warpage during wave soldering. During wave soldering, when the pallet absorbs heat from the solder wave, only a portion of the heat is absorbed by PCB. This method can minimize PCB warpage, but the pallet is warped or twisted when it is exposed to high temperature. The pallet design and material used are important to solve this problem.

The parametric design of the PCB, including its mass, size, component density, and component type, influences the control over the wave soldering process (Coit and Smith, 1995). Different component configurations affect the temperature distribution and thermal profile of PCBs. Visualizing the PCB temperature contour, heat transfer coefficient, and stress during the process is difficult because of limited equipment. The coupling of different solvers yields an effective model of the process phenomenon through the exchange of temperature and heat transfer coefficient data from the thermal fluid and structural analyses (Lau et al., 2012a).

In the wave soldering process, the PCB experience different thermal expansions (CTEs). This situation leads the PCB to the manufacturing defects and fatigue during the field operations (Guo, 1995). Adding anti-oxidation elements in solder alloys improve oxidation resistance but results in poor wettability in low silver lead-free solder (Wang

et al., 2013). A combination of many factors in the PCB design and process require proper process control in the wave soldering process. As aforementioned, the PCB warpage would induce unintended defects on the component and solder joint, which may cause the malfunction of the electronic devices. Therefore, the minimization of the PCB warpage is crucial to eliminate the solder joint defects.

2.7 Optimization- Response surface methodology (RSM)

An optimization is a fundamental and systematically applied in most electronic assembly industries, for example response surface methodology (RSM) (Chansa-ngavej and Kasemsomporn, 2010), genetic algorithm (GA) (Huang and Hung, 2008), and neuro-fuzzy genetic algorithm (Chiang and Su, 2003). Physical design and assembly condition such as pin size, PCB hole diameter, pin position and angle may influence the molten solder flow characteristic during the wave soldering process. A process setting such as solder temperature, conveyor speed and molten solder fountain may influence the quality of the solder joint. For example, high temperatures could result in overheating of the PCB and components attached to the PCB. This situation may yield unintended defects and reduce the overall reliability. An optimized wave soldering setting, which yields optimum product quality and reliability, is essential in PCB assembly. Various optimization methods such as Taguchi method (Barbini et al., 2007; Mach et al., 2010), mixed-level fractional design (Mesenbrink et al., 1994), expert system using self-organizing maps and quality-oriented optimization (Liukkonen et al., 2009; 2011b), the neural network approach (Coit et al., 1998; 1994), and DOE (Arra et al., 2002) have been applied to optimize the productivity, quality, and reliability of the wave soldering process. The optimization of the wave soldering process is also